Plant Biotechnology 30, 365–373 (2013)
DOI: 10.5511/plantbiotechnology.13.0527a

Original Paper

CAD2 deficiency causes both *brown midrib* and *gold hull and internode* phenotypes in *Oryza sativa* L. cv. Nipponbare

Taichi Koshiba[1], Shinya Murakami[1], Takefumi Hattori[1,a], Mai Mukai[1], Akira Takahashi[2], Akio Miyao[2], Hirohiko Hirochika[2], Shiro Suzuki[1], Masahiro Sakamoto[3], Toshiaki Umezawa[1,4,*]

[1] Research Institute for Sustainable Humanosphere, Kyoto University, Uji, Kyoto 611-0011, Japan; [2] National Institute of Agrobiological Science, Tsukuba, Ibaraki 305-8602, Japan; [3] Graduate School of Agriculture, Kyoto University, Kyoto 606-8502, Japan; [4] Institute of Sustainability Science, Kyoto University, Uji, Kyoto 611-0011, Japan
* E-mail: tumezawa@rish.kyoto-u.ac.jp Tel: +81-774-38-3625 Fax: +81-774-38-3682

Received December 17, 2012; accepted May 27, 2013 (Edited by Y. Ozeki)

Abstract Several *brown midrib* (*bm*) mutants have so far been isolated from the C4 grasses, maize, sorghum and pearl millet, but have not been detected in C3 grasses including rice (*Oryza sativa*). In the present study we characterized the *cad2* (*cinnamyl alcohol dehydrogenase 2*) null mutant isolated from retrotransposon *Tos17* insertion lines of *Oryza sativa* L. ssp. *japonica* cv. Nipponbare. This mutant exhibited brown-colored midribs in addition to hulls and internodes, clearly indicating both *bm* and *gold hull and internode* (*gh*) phenotypes. The enzymatic saccharification efficiency in the culm of *cad2* null mutant was increased by 16.1% than that of the control plants. The lignin content of the *cad2* null mutant was 14.6% lower than that of the control plants. Thioacidolysis of the *cad2* null mutant indicated the presence of cinnamaldehyde structures in the lignin. Taken together, our results show that deficiency of *OsCAD2* causes the *bm* phenotype in addition to *gh*, and that the coloration is probably due to the accumulation of cinnamaldehyde-related structures in the lignin. Additionally, this *cad2* null mutant was useful to silage purposes and biofuel production.

Key words: *Brown midrib*, lignin, cinnamyl alcohol dehydrogenase, *gold hull and internode*, rice.

Lignin is a complex phenylpropanoid polymer, and is biosynthesized via oxidative coupling of *p*-hydroxycinnamyl alcohols (monolignols) and related compounds that are formed in the cinnamate/monolignol pathway (Umezawa 2010). Lignin fills the spaces between cell wall polysaccharides and confers mechanical strength and imperviousness to the cell wall (Boerjan et al. 2003). Therefore, lignin biosynthesis is closely related to the evolution of land plants.

Lignin has several properties that present obstacles to chemical pulping, forage digestion, and enzymatic hydrolysis of plant cell wall polysaccharides for biorefining. For these processes, it would be beneficial for plant materials to either have less lignin, or to have lignin that is easier to remove. Mutant plants in which genes encoding lignin biosynthetic enzymes are down-regulated are generally expected to have lower lignin content and higher enzymatic saccharification efficiency. For these reasons, lignin biosynthesis is an area of great interest (Chiang 2006; Dixon and Reddy 2003; Vanholme et al. 2008; Weng et al. 2008).

Several *brown midrib* (*bm* or *bmr* for sorghum) mutants have been isolated in maize (*Zea mays*), sorghum (*Sorghum bicolor*), and pearl millet (*Pennisetum glaucum*) arising by either spontaneous or chemical mutagenesis (Barrière et al. 2004; Cherney et al. 1991; Sattler et al. 2010). The characteristic reddish-brown to tan colored midribs of the mutant leaf blades contrasts with the pale green midribs of the wild type. In addition, the mutants show similar coloration in stalks and generally have reduced lignin content and higher in vitro digestibility compared with wild-type plants. Hence, the mutants have been receiving a lot of interest in relation not only to silage purposes (Barrière et al. 2004; Cherney et al. 1991; Sattler et al. 2010), but also biofuel production (Sattler et al. 2010).

In maize, six *bm* (*bm1* through *bm6*) loci have been identified to date (Ali et al. 2010; Sattler et al. 2010).

Abbreviations: 4CL, 4-hydroxycinnamate CoA ligase; *bm*, *brown midrib*; CAD, cinnamyl alcohol dehydrogenase; CAOMT, caffeic acid *O*-methyltransferase; CCoAOMT, caffeoyl CoA *O*-methyltransferase; CCR, cinnamoyl CoA reductase; *gh*, *gold hull and internode*; H/V, *p*-hydroxybenzaldehyde/vanillin; S/V, syringaldehyde/vanillin; WT, wild type; TLC, thin-layer chromatography

[a] Present address: Institute of Socio-Arts and Sciences, The University of Tokushima, 1-1 Minamijosanjima-cho, Tokushima 770-8502, Japan.

This article can be found at http://www.jspcmb.jp/
Published online September 5, 2013

It was concluded that *bm1* is not a null mutation of *ZmCAD2*, but affects its expression, possibly through alteration in upstream or downstream non-coding regions (Halpin et al. 1998). Later, Guillaumie et al. reported that *bm1* was probably in a gene that regulates the expression of the *ZmCAD* gene family (Guillaumie et al. 2007). On the other hand, the *bm3* mutation was found to occur in the gene encoding caffeic acid *O*-methyltransferase (ZmCAOMT) (Morrow et al. 1997; Vignols et al. 1995). In addition, downregulation of CAOMT in maize using sorghum *CAOMT* resulted in a *bm* phenotype (He et al. 2003).

In sorghum, at least four independent *brown midrib* loci were established, which were represented by *bmr2*, *bmr6*, *bmr12*, and *bmr19* (Saballos et al. 2008). The abbreviation *bmr* was adopted to distinguish it from *bm*, already in use for the sorghum *bloomless* mutants (Saballos et al. 2009). *SbCAD2* was found to be responsible for the phenotype of the *bmr6* mutants (Saballos et al. 2009; Sattler et al. 2009), while the *bmr12* mutation was found to be located in the gene encoding SbCAOMT (Bout and Vermerris 2003). Similar coloration was observed in a gymnosperm tree; a mutant pine (*Pinus taeda*) deficient in CAD showed brown colorlation in the wood (MacKay et al. 1997).

In addition to *bm* mutants, some transgenic plants in which genes encoding enzymes in the cinnamate/monolignol pathway were downregulated showed unusual red, brown or orange colorlation, which was not observed in the corresponding wild-type plants. For example, *CAOMT* downregulation in poplar (*Populus tremula* × *Populus alba*) (Van Doorsselaere et al. 1995) and in aspen (*Populus tremuloides*) (Tsai et al. 1998) resulted in xylem tissues with pale rose and reddish brown coloration, respectively. *CAD* downregulation in alfalfa (*Medicago sativa*) (Baucher et al. 1999), tobacco (*Nicotiana tabacum*) (Chabannes et al. 2001; Halpin et al. 1994; Hibino et al. 1995), and poplar (*P. tremula*×*P. alba*) (Baucher et al. 1996) resulted in various red, brown and pink colorations of the xylem. With *CCR* downregulation, brown (Chabannes et al. 2001) and orange-brown (Piquemal et al. 1998) coloration was observed in the xylem of transgenic tobacco plants (*N. tabacum*). In addition, brown colorlation in the xylem of *4CL*-downregulated tobacco (*N. tabacum*) (Kajita et al. 1996) and red coloration of xylem of *CCoAOMT*-downregulated poplar (*P. tremula*×*P. alba*) (Zhong et al. 2000) were reported.

The mechanisms for this coloration in the mutants have not been fully elucidated. However, the red-purple coloration of the *CAD*-downregulated tobacco has been attributed to the incorporation of hydroxycinnamaldehydes into lignin (Hibino et al. 1995), because a synthetic lignin, a dehydrogenation polymer from coniferaldehyde, exhibited red-purple, wine-red like coloration (Higuchi et al. 1994), and because hydroxycinnamaldehyde contents in the mutants are significantly elevated compared with the corresponding wild-type plants (Barrière et al. 2004; Sattler et al. 2009). Similarly, the red-brown coloration of transgenic aspen (*P. tremuloides*) in which *CAOMT* was downregulated was also ascribed to a higher amount of coniferaldehyde residues in the transgenic line (Tsai et al. 1998).

Interestingly, no *bm* mutants have been identified or described for the C3 grasses including rice (*Oryza sativa*) which is another important Gramineae crop (Sattler et al. 2010), although CAD-deficient rice mutants (Ookawa et al. 2008; Zhang et al. 2006) and *CAD*-downregulated rice (Shiba et al. 2007) were described. It has been suggested for reasons yet to be determined that C3 grasses do not accumulate the characteristic light-brown pigment in the midribs of their leaf blades (Sattler et al. 2010). A point mutation of *OsCAD2* gene in *O. sativa* L. ssp. *indica* cv. Zhefu802 (hereafter referred to as Zhefu802) exhibited an obvious reddish-brown pigment in the internode, and basal leaf sheath at the heading stage and golden yellow coloration of the hull, and designated as the *gold hull and internode* (*gh*) *2* mutant (Zhang et al. 2006). Another *gh2* mutant of an unknown background showed lower *OsCAD2* gene expression and lignin content compared with a control rice plant (Ookawa et al. 2008). In addition, Oryzabase (http://www.shigen.nig.ac.jp/rice/oryzabaseV4/) shows a number of rice *gh* mutants (*gh1*, *gh2*, and *gh3*). For example, a *gh2* mutant of *O. sativa* L. ssp. *japonica* cv. Miyazaki No.1 was reported by Iwata and Omura (1971), while recently a *gh1* mutant was found to be due to a mutation of a chalcone isomerase gene (*OsCHI*; Os03g0819600) involved in the flavonoid biosynthesis (Hong et al. 2012). Again, however, none of the *gh* mutants were reported to show the *bm* phenotype.

Rice straw, together with other inedible lignocellulosic biomass products such as corn stover, sugarcane bagasse, and wheat straw, is expected to be a promising feedstock as an industrial fermentation substrate (Park et al. 2011). In Japan, annual domestic production of rice straw accounts for about 9.6 Mt. However, more than 60% of rice straw is deposited on rice fields (Park et al. 2011). In addition, rice is an important model plant for large-sized Gramineae bioenergy plants, such as *Erianthus*, napier grass, and switch grass (Yamamura et al. 2013). Hence, many research projects for bioconversion of rice straw to fermentable carbohydrates are on-going in Japan (Park et al. 2011). In this bioconversion, enzymatic saccharification of lignocellulosic materials is the key step, and is affected largely by the amount and structure of lignins. In this context, we characterized a rice mutant which had a *Tos17* insertion into *CAD2* gene and found that the mutant exhibits higher enzymatic saccharification efficiency and the *bm* phenotype as well as the *gh2* phenotype.

Materials and methods

Plants

The *gh2* mutant line (NE4246) was identified among the *Tos17* insertion mutant population derived from *O. sativa* L. ssp. *japonica* cv. Nipponbare. Mutagenesis with *Tos17* and polymerase chain reaction (PCR) screening of mutants were performed as described by Kumar and Hirochika (2001) and Miyao et al. (2003). The homozygous *gh2* mutant and *GH2* sibling plants and the wild type were cultivated in both the test field of the National Institute of Agrobiological Science and the green house facility of the Research Institute for Sustainable Humanosphere, Kyoto University.

Tos17 insertion at the *GH2* gene locus in the *gh2*/*gh2* mutant and no insertion in the *GH2*/*GH2* plant were confirmed by genomic PCR analysis (Figure 1). Total DNA was extracted from leaf blades with a DNeasy plant mini kit (Qiagen, Hilden, Germany), and PCR was done with total DNA as the template and three primers [*OsCAD2* 1st intron fwd (P1): 5′-TGC TAT GCA ATT CTC GTG CCA TGC-3′, *OsCAD2* 2nd exon rev (P2): 5′-TTC TTG GCC TGG TGG ATG TCA GTA-3′, P3: 5′-CAG CAA CGA TGT AGA TGG TCA AGC-3′]. The PCR products were analyzed on a 1% (w/v) agarose gel and were visualized with ethidium bromide. An *OsCAD2* (Os02g0187800) RNA-interference (RNAi) knock-down plant was prepared previously (Hattori et al. 2012) using the specific primer set: *CAD2*_RNAi_f, 5′-CAC CAA GAC TGG GCC TGA AGA TGT-3′ and *CAD2*_RNAi_r, 5′-CGG GAT CTT CAC CAC AAA CT-3′.

qRT-PCR analysis

Total RNA was extracted from each part of rice plants with an RNeasy plant mini kit (Qiagen). First-strand cDNA was synthesized in a 20 μl reaction mixture containing 1 μl of SuperScript II Reverse Transcriptase (Invitrogen, Carlsbad, CA, USA), 1 μg of total RNA, 50 pmol Oligo(dT)$_{20}$ primer (Invitrogen), 10 nmol dNTPs, 0.2 μM DTT, and 1 μl of RNaseOUT (Invitrogen) at 42°C for 50 min. The reaction mixture was diluted 8-fold with TE buffer (pH 8.0).

Quantitative real-time RT-PCR (qRT-PCR) was conducted using an Applied Biosystems 7300 Real-time PCR System. For each reaction, the 20 μl mixture contained 1 μl of first-strand cDNA, 12.5 μl of Power SYBR Green PCR Master Mix (Applied Biosystems, Foster City, CA), and 2 pmol each of the forward and reverse primers: *CAD2* fwd, 5′-TGT GTG AGA CTC TGA CGA CTT GTC-3′ and *CAD2* rev, 5′-CAT ATA TTG CGA GGC CGA ATT T-3′. The amplification program was as follows: 50°C for 2 min, 95°C for 10 min and 40 cycles at 95°C for 15 s and 60°C for 1 min (Suzuki et al. 2006). Single fluorescence reading was performed at each cycle immediately following the elongation period at 60°C. The fluorescence was measured during the cycle to ensure single product amplification. Cycle threshold (Ct) values were determined automatically using the Sequence Detection Software ver. 1.2 (Applied Biosystems). Each reaction was conducted in triplicate. A ubiquitin gene (*OsUBQ5*; accession no. AK061988) was amplified using specific primers (*UBQ5* fwd, 5′-ACC ACT TCG ACC GCC ACT ACT-3′ and *UBQ5* rev, 5′-ACG CCT AAG CCT GCT GGT T-3′) as an internal control. The ΔΔCt method was adopted for calculation of gene expression (User Bulletin #2, Applied Biosystems).

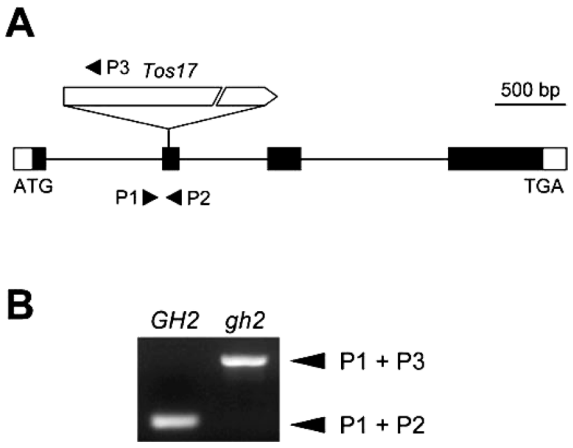

Figure 1. Identification and confirmation of the *Tos17* insertion mutant. (A) Schematic diagram of the *OsCAD2* gene (Os02g0187800) and the retrotransposon *Tos17* insertion site in the allele. Black boxes indicate exons encoding the protein, and open boxes indicate the 5′ and 3′ UTR regions. Solid lines represent introns, and arrowheads indicate the primer annealing sites. (B) Confirmation of the *Tos17* insertion in the *GH2* (control) and the *gh2* mutant with three primers, P1, P2 and P3. Genomic DNA extracted from each individual was used as the template for PCR. The *GH2* genome shows no *Tos17* insertion, while the *gh2* mutant shows homozygous *Tos17* insertion.

Histochemical analysis

Fresh hand-cut sections (approximately 100 μm-thick) were prepared from the third internodes of rice plants at the heading stage. For Wiesner staining, the sections were incubated for 10 min in phloroglucinol solution (1% in 70% ethanol), and treated with 18% HCl for 5 min. The sections were photographed under a light microscope (Olympus BX-51, Olympus, Tokyo, Japan) (Li et al. 2009; Zhang et al. 2006).

Milling of the tissues

Dried rice plants after removal of spikelets were separated to the following tissues [total fraction without spikelets (T), leaf blades (LB), leaf sheaths (LS), internodes without uppermost internodes (IN), uppermost internodes (U), tissues around ±5 mm from nodes (N), rachises and panicle branches without spikelets (R)]. These tissues were cut into about 5-mm pieces and dried in a desiccator at room temperature with silica gel. They were further dried in vacuo overnight at room temperature. Each dried sample (0.5 g) was ground in a ball mill (TissueLyser, Qiagen) with 20 mm stainless steel balls at 26 Hz for 3 min (T, U, N, R), 2 min (LB, LS), or 4 min (IN). The milled rice materials were put into glass bottles and stored in a desiccator with silica gel at room temperature until use.

Determination of enzymatic saccharification efficiency

Enzymatic saccharification efficiency was determined by the method of Hattori et al. (2012). Briefly, the starch in the tissue (T) was degraded using a Total Starch Kit (Megazyme, Co. Wicklow, Ireland). The starch-free residue (SFR) was separately subjected to acid saccharification and enzymatic saccharification using enzymes including Celluclast 1.5 L (cellulase), Novozyme 188 (cellobiase), and Ultraflo L (β-glucanase and xylanase with side activities of cellulase, hemicellulase, and pentosanase) (Novozymes, Bagsvaerd, Denmark). In the enzymatic saccharification of SFR, the amounts of glucose liberated were determined at 1, 2, 3, 6, 8, 10, 12, 14, 20, 24, and 48 h from the start. The enzymatic saccharification efficiency (%) was determined by the following equation:

$$\text{Enzymatic saccharification efficiency (\%)} = \frac{\text{Enzymatically hydrolysable glucan-derived glucose from SFR}}{\text{Glucan-derived glucose by acid saccharification from SFR}} \times 100$$

Preparation of coniferaldehyde dehydrogenation polymer

Synthetic lignin [dehydrogenation polymer (DHP)] was prepared by peroxidase-catalyzed polymerization of coniferaldehyde. Coniferaldehyde was prepared according to Nakamura and Higuchi (1976), ^{1}H-NMR δ ($CDCl_3$) 3.95 (3H, s), 6.59 (1H, dd, *J* 7.75, 15.80), 6.95 (1H, d, *J* 8.14), 7.06 (1H, d, *J* 1.82), 7.12 (1H, dd, *J* 1.83, 8.21), 7.40 (1H, d, *J* 15.79), 9.64 (1H, d, *J* 7.76), which was taken by a Varian XL-200 FT-NMR spectrometer (Varian, Palo Alto, CA, USA). Coniferaldehyde thus obtained (10 mg) was dissolved in 0.1 ml of acetone, and mixed with 1 ml of 0.05 M acetate buffer (pH 5.2). Separately prepared 10 μl of horse radish peroxidase solution dissolved in 0.05 M acetate buffer (pH 5.2, 1 mg ml^{-1}) and 10 μl of 3% H_2O_2 were added to the reaction mixture. After 5 min at room temperature in the dark, 10 μl of 3% H_2O_2 was added and the reaction was continued for an additional 5 min in the same way. The reaction was stopped by adding 1.5 ml of ethyl acetate (EtOAc). The synthesized DHP was collected by centrifugation, washed with water for three times, and dried in vacuo.

Lignin analysis

Lignin content in each tissue (T), (LB), (LS), (U), (IN), (N), and (R) was determined using the thioglycolic acid lignin method (Suzuki et al. 2009). The aromatic ring composition of lignin was analyzed by a microscale protocol of the nitrobenzene oxidation method (Yamamura et al. 2010; Yamamura et al. 2011). Thioacidolysis of lignin and DHP was conducted as previously described (Nakatsubo et al. 2008; Yamamura et al. 2011). For detecting the cinnamaldehyde specific-indene compound, the thioacidolysis products from the hulls of *gh2* mutant and DHP were individually separated by preparative silica gel TLC (EtOAc : *n*-hexane, 1 : 2), and submitted to GC-MS analysis. GC-MS was performed using a Shimadzu QP-5050A GCMS system (Shimadzu Co., Ltd., Kyoto, Japan). The GC-MS conditions were as follows: Shimadzu Hicap CBP10-M25-025 column (25 m×0.22 mm); carrier gas, helium; injection temperature, 230°C; oven temperature, 40°C at *t*=0 to 2 min, then to 230°C at 40°C min^{-1}; ionization, electron-impact mode (70 eV) (Nakatsubo et al. 2008; Yamamura et al. 2011).

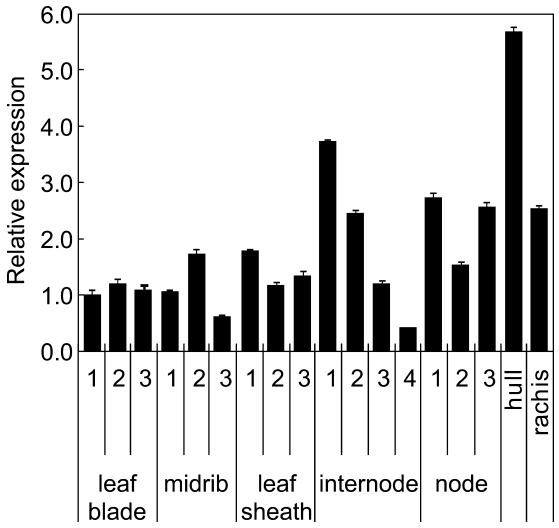

Figure 2. Expression level of *OsCAD2* in different tissues of wild-type plants. The tissues include leaf blades, midribs, leaf sheathes, internodes, nodes, hulls and rachises at the heading stage. The numbers 1, 2 and 3 in above "leaf blade", "midrib" and "leaf sheath" indicates the flag leaf, second youngest leaf and third youngest leaf, respectively. The numbers above "internode" and "node" indicate the corresponding first, second, third and fourth internode or node, respectively. The leaf blades did not include midribs. Each value is the mean of three replicates±SD, and expressed relative to the expression in leaf blade No. 1.

Results

In the wild type of *O. sativa* L. ssp. *japonica* cv. Nipponbare (hereafter referred to as Nipponbare), *cinnamyl alcohol dehydrogenase 2* gene [*CAD2* (an ortholog of the *GH2* in Zhefu802), Os02g0187800)] was expressed widely in all the tissues tested (Figure 2). We screened the *Tos17* mutant panel and isolated a plant that had a retrotransposon insertion in the second exon of the gene (Figure 1). Homozygous *gh2* mutant exhibits obvious reddish-brown color in the panicles (hulls), internodes, and nodes at the heading stage (Figure 3), in which relatively high expression of *OsCAD2* (=*GH2*) gene was observed (Figure 2). These phenotypes were typical of *gh2* mutant of Zhefu802 (Zhang et al. 2006). Except for the reddish-brown coloration in these specific tissues, the *gh2* mutant of Zhefu802 showed similar development to the wild type, and the *bm* phenotype was not reported (Zhang et al. 2006).

In sharp contrast, the present *gh2* mutant clearly showed the *bm* phenotype as indicated in Figure 3

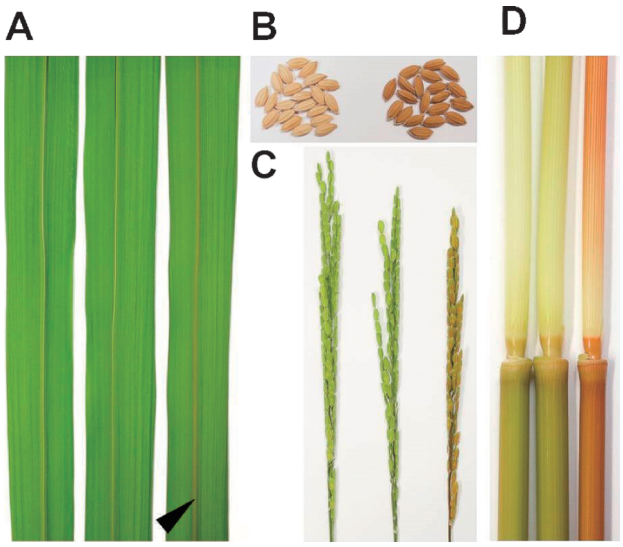

Figure 3. The *gh2* mutant presented a *brown-midrib* phenotype. (A) The flag leaves of WT (left), *GH2* (middle), and *gh2* (right) plants at the heading stage. The arrowhead indicates the reddish-brown coloration of the midrib in the *gh2* mutant. (B) The grains of *GH2* (left) and *gh2* (right) plants at maturation. (C) The panicles of WT (left), *GH2* (middle), and *gh2* (right) plants at the heading stage. (D) The culms of WT (left), *GH2* (middle), and *gh2* (right) plants at the heading stage.

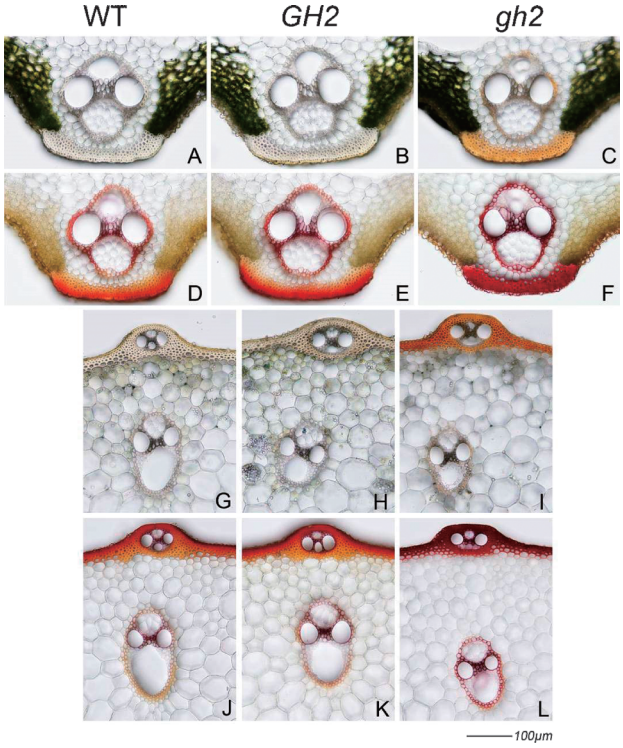

Figure 4. Histochemical analysis of WT, *GH2*, and *gh2* plants. Transverse sections of flag leaves (A–F) and third internodes (G–L) from WT (left column), *GH2* (middle column), and *gh2* (right column) plants were photographed under a microscope. (A–C, G–I) Transverse sections without staining. (D–F, J–L) Transverse sections with staining by Wiesner reagent. Reddish-brown pigment was deposited in the walls of sclerenchyma cells and vascular bundle cells of flag leaves (C) and internodes (I) from *gh2* plants. Enhanced staining with Wiesner reagent was observed in the regions in which the reddish-brown pigment was accumulated in *gh2* plants (F, L). The dots seen in the intracellular spaces of (G), (H), and (I) were starch granules.

(arrowhead). The reddish-brown pigment was observed in the sclerenchyma and vascular bundle cell walls in the leaf and culm (Figure 4C, I). In addition, histochemical staining with Wiesner reagent indicated enhanced red-purple coloration in the leaf midribs and internodes of the *gh2* mutant compared with those of the control plants (wild-type and *GH2* plants) (Figure 4). Furthermore, the RNAi technique successfully downregulated the

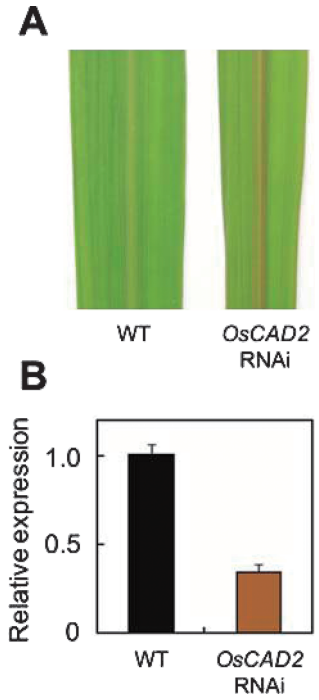

Figure 5. The phenotype of transgenic *OsCAD2*-knockdown (*OsCAD2* RNAi) plant. (A) The midrib of flag leaves in WT (left) and *OsCAD2* RNAi (right) plants at the heading stage. (B) The *OsCAD2* expression levels of flag leaves in WT and *OsCAD2* RNAi plants at the heading stage were measured by real-time RT-PCR. Each value is the mean of three replicates±SD.

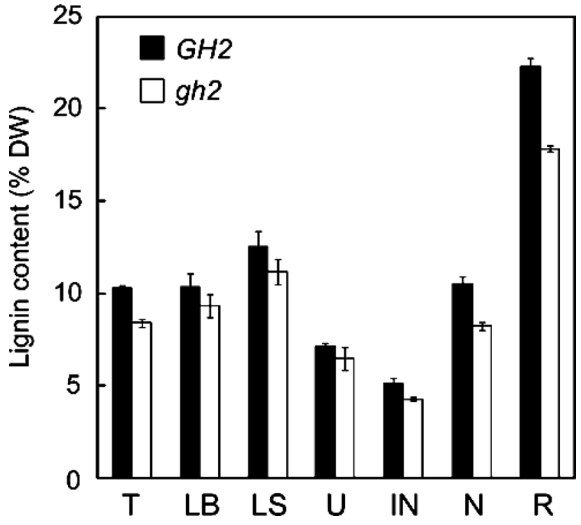

Figure 6. Thioglycolic acid lignin content in tissues of *GH2* and *gh2* plants. Each value is the mean of three replicates±SD. T, total fraction without spikelets; LB, leaf blades; LS, leaf sheaths; U, uppermost internodes; IN, internodes without uppermost internodes; N, tissues around ±5 mm from nodes; R, rachises and panicle branches without spikelets. DW, dry weight.

expression of the *OsCAD2* gene as shown in Figure 5B, and the knock-down plant exhibited reddish-brown coloration in the midrib, i.e. the *bm* phenotype (Figure 5A).

When the Klason method is applied for rice lignin quantitation, it results in erroneous values due to high silica content (Lai and Sarkanen 1971). Hence, we employed the thioglycolic acid method (Suzuki et al. 2009). In all of the tissues tested, the *gh2* mutant had 10–20% less lignin than control (*GH2*) plants (Figure 6). The *gh2* mutant and control (*GH2*) plants were then subjected to lignin structural analyses using the thioacidolysis and nitrobenzene oxidation methods. The former method detected not only trithioethylphenyl compounds which are specifically formed from *β-O*-4 lignin substructures, but also the cinnamaldehyde specific-indene compound (Kim et al. 2002). The indene compound [trimethylsilyl-8G (Figure 7) described in Kim et al. (2002)] was detected from thioacidolysis products of hulls of *gh2* mutant with mass spectra: MS, *m*/*z* (%) 354 (M^+, 87), 325 (26), 293 (100), 260 (57), 230 (27), which is in accordance with the literature data [MS, *m*/*z* (%) 354 (M^+, 100), 325 (18), 293 (76), 260 (35), 230 (12)] (Table 1; Kim et al. 2002). Furthermore, this product was also detected when the synthetic lignin (DHP) prepared by polymerization of coniferaldehyde was subjected to thioacidolysis: MS, *m*/*z* (%) 354 (M^+, 83), 325 (28), 293 (100), 260 (58), 230 (32). On the other hand, the indene compound was not detected in the thioacidolysis products from the control (*GH2*) plants (Table 1). These results indicated the occurrence of coniferaldehyde residues in the lignin of the *gh2* mutant. Nitrobenzene oxidation analysis showed that the aromatic composition of the *gh2* mutant lignin was slightly modified, as evidenced by lower S/V and H/V values throughout the three organs: flag leaf, culm, and hull (Table 2).

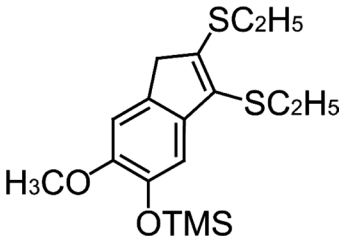

Figure 7. The structure of compound 8G (2,3-bis-ethylsulfanyl-6-methoxy-1*H*-inden-5-ol) (trimethylsilyl ether). TMS, trimethylsilyl.

Table 1. Formation of 8G.

	IS	8G*
GH2	100	N.D.
gh2	100	168.32

* Relative value to IS (internal standard, docosane). N.D.: not detected.

Figure 8 shows the enzymatic saccharification efficiency in the tissue (T) of *gh2* mutant and control (*GH2*) plants. The efficiency of saccharification after 48 h incubation was 35.0% in the control plants, while it reached to 40.6% in the *gh2* mutants (Figure 8). The amounts of glucose liberated by acid saccharification

Table 2. Lignin aromatic ring compositions by nitrobenzene oxidation in the flag leaf, culm, and hull of *GH2* and *gh2* plants.

		Flag leaf	Culm	Hull
			μmol g^{-1} cell wall residue	
Vanillin (V)	*GH2*	94.31±2.56	130.64±8.92	354.36±13.24
	gh2	77.83±4.98*	114.54±3.38*	211.28±3.92*
Syringaldehyde (S)	*GH2*	16.44±0.62	49.91±1.52	35.32±1.62
	gh2	9.16±0.89*	30.72±2.61*	16.51±1.50*
p-Hydroxybenzaldehyde (H)	*GH2*	20.05±0.31	57.83±8.25	55.83±2.97
	gh2	14.99±0.50*	24.22±2.13*	24.83±0.36*
S/V	*GH2*	0.17±0.01	0.38±0.02	0.10±0.00
	gh2	0.12±0.01*	0.27±0.02*	0.08±0.01*
H/V	*GH2*	0.21±0.01	0.44±0.04	0.16±0.00
	gh2	0.19±0.01*	0.21±0.01*	0.12±0.00*

Each value is the mean of three replicates±SD. Asterisks indicate significant difference from the *GH2* plant (Student's *t*-test, $p<0.05$). S/V and H/V: Molar ratios of S to V and H to V, respectively.

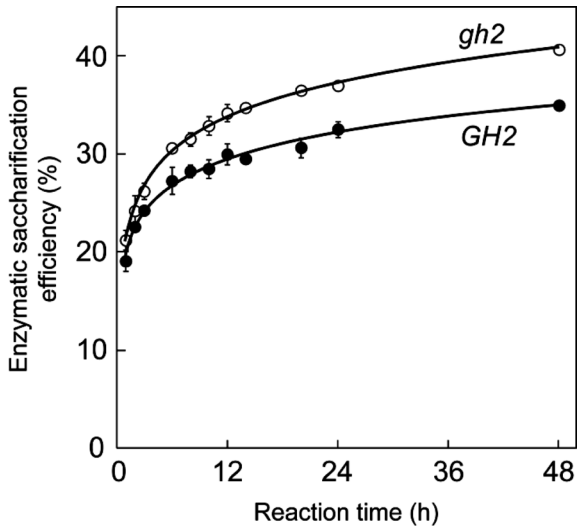

Figure 8. Enzymatic saccharification efficiency in the shoots of *GH2* and *gh2* plants over 48 h. Each value is the mean of three replicates±SD.

from cell wall residues of *gh2* mutant (31.0±1.8% cell wall residue) did not differ significantly with those form control (*GH2*) plants (30.1±1.0% cell wall residue).

Discussion

In the present study we have demonstrated that a null *gh2* mutant [*gh2*/*gh2* (−/−)] isolated from a *Tos17* mutant panel population of Nipponbare showed a clear *bm* phenotype in addition to the typical *gh* phenotype. The corresponding *GH2* [*GH2*/*GH2* (+/+)] (Figure 3A) and heterozygous [*gh2*/*GH2* (−/+)] (data not shown) plants showed a normal green midrib phenotype. Although each *Tos17* mutant line harbors a number of retrotransposon insertions (Kumar and Hirochika, 2001; Miyao et al. 2003), a transgenic plant in which the expression of the *OsCAD2* (*GH2*) gene was downregulated by the RNAi technique also exhibited red-purple coloration in the midrib (Figure 5). Taken together, these results unequivocally show the occurrence of a *gold hull and internode* (*gh*)/*brown midrib* (*bm*) phenotype, and it was confirmed that this phenotype is due to the impaired *OsCAD2* expression. This is the first description of a *bm* phenotype in a typical C3 grass, in this case rice.

The wild-type Nipponbare showed significant *GH2* gene expression in the midrib (Figure 2), which was probably strong enough to cause the *bm* phenotype in the corresponding *gh2* mutant. By contrast, in the wild-type Zhefu802, the expression of the *GH2* gene in the midribs was lower than that in the hulls which exhibit a reddish brown pigment in the *gh2* mutant, while the total CAD activity in the midribs was higher than that in the hulls (Zhang et al. 2006). These data suggest that OsCAD2 was not major in the midribs of the wild-type Zhefu802. This can account for the reason why no *bm* phenotype was observed in the *gh2* mutant of the Zhefu802.

Histochemical staining with Wiesner reagent indicated the red-purple coloration was greater in the *gh2* mutant than in the control plant, strongly suggesting the occurrence of cinnamaldehyde residues in the mutant, which is a typical characteristic of *CAD*-deficient mutants or transgenic plants (Barrière et al. 2004; Kim et al. 2003; Ralph et al. 2001; Sattler et al. 2010). This was further confirmed by the detection of a degradation fragment derived from the cinnamaldehyde structure; thioacidolysis of the *gh2* mutant detected a cinnamaldehyde-specific degradation product, i.e. the indene compound (Kim et al. 2002) (Figure 7; Table 1), from the hull, while the compound was not detected in the control (*GH2*) plants (Table 1).

All of the tested tissues of the *gh2*/*bm* mutant of Nipponbare had 10–20% less lignin than the control (*GH2*) plants (Figure 6). These reductions were greater than those previously reported for the *gh2* mutant of the Zhefu802 (*gh2* mutant: 14.2%, wild type: 15.0% in the internodes) (Zhang et al. 2006). As shown in Figure 8, the reduction of lignin levels significantly affected the enzymatic saccharification efficiency of the lignocelluloses in the *gh2* mutant. After enzymatic

incubation for 48 h, saccharification efficiency in the control (*GH2*) plants reached 35.0%, while in the *gh2* plants was 40.6%, which is about 16.1% higher than that in the control plants. These results clearly indicate that rice *gh2*/*bm* mutants are promising for fodder and feedstock as an industrial fermentation substrate. Importantly, the mutation in the Nipponbare can be exploited to breed rice cultivars by cross-fertilization, especially forage paddy rice cultivars.

In conclusion, the *cad2* (*cinnamyl alcohol dehydrogenase 2*) null mutant isolated from retrotransposon *Tos17* insertion lines of Nipponbare showed the *bm* phenotype in addition to the *gh* phenotype. This is the first report of a *bm* mutant from C3 grasses. The *gh2*/*bm* mutant had higher enzymatic saccharification efficiency and lower lignin content compared with the control (*GH2*) plant. This mutation could be applied to breed forage paddy rice cultivars that are suitable for use as fodder and industrial feedstock.

Acknowledgements

The authors thank Ms. Aiko Morita, Ms. Kumiko Murata, Ms. Mayumi Inutsuka, and Ms. Sawako Ohtsu for their technical assistance. Thanks are due to Professor Ko Shimamoto, Nara Institute of Science and Technology, for the supply of pANDA vector; and Novozymes, Bagsvaerd, Denmark, for the supply of Celluclast 1.5 L, Novozyme 188, and Ultraflo L. This research was partly supported by a grant from the Ministry of Agriculture, Forestry and Fisheries of Japan (Genomics for Agricultural Innovation, GMA-0006). A part of this study was conducted using the Development and Assessment of Sustainable Humanosphere/Forest Biomass Analytical System at the Research Institute for Sustainable Humanosphere, Kyoto University, Japan.

References

Ali F, Scott P, Bakht J, Chen Y, Lubberstedt T (2010) Identification of novel brown midrib genes in maize by tests of allelism. *Plant Breed* 129: 724–726

Barrière Y, Ralph J, Méchin V, Guillaumie S, Grabber JH, Argillier O, Chabbert B, Lapiere C (2004) Genetic and molecular basis of grass cell wall biosynthesis and degradability. II. Lessons from brown-midrib mutants. *C R Biol* 327: 847–860

Baucher M, Bernard-Vailhé MA, Chabbert B, Besle J-M, Opsomer C, Van Montagu M, Botterman J (1999) Down-regulation of cinnamyl alcohol dehydrogenase in transgenic alfalfa (*Medicago sativa* L.) and the effect on lignin composition and digestibility. *Plant Mol Biol* 39: 437–447

Baucher M, Chabbert B, Pilate G, Van Doorsselaere G, Tollier M-T, Petit-Conil M, Cornu D, Monties B, Van Montagu M, Inzé D, et al. (1996) Red xylem and higher lignin extractability by down-regulating a cinnamyl alcohol dehydrogenase in poplar. *Plant Physiol* 112: 1479–1490

Boerjan W, Ralph J, Baucher M (2003) Lignin biosynthesis. *Annu Rev Plant Biol* 54: 519–546

Bout S, Vermerris W (2003) A candidate-gene approach to clone the sorghum *Brown midrib* gene encoding caffeic acid *O*-methyltransferase. *Mol Genet Genomics* 269: 205–214

Chabannes M, Barakate A, Lapierre C, Mrita JM, Ralph J, Pean M, Danoun S, Halpin C, Grima-Pettenati J, Boudet AM (2001) Strong decrease in lignin content without significant alteration of plant development is induced by simultaneous down-regulation of cinnamoyl CoA reductase (CCR) and cinnamyl alcohol dehydrogenase (CAD) in tobacco plants. *Plant J* 28: 257–270

Chiang VL (2006) Monolignol biosynthesis and genetic engineering of lignin in trees, a review. *Environ Chem Lett* 4: 143–146

Cherney JH, Cherney DJR, Akin DE, Axtell AD (1991) Potential of brown-midrib low-lignin mutants for improving forage quality. *Adv Agron* 46: 157–198

Dixon RA, Reddy MSS (2003) Biosynthesis of monolignols. Genomic and reverse genetic approaches. *Phytochem Rev* 2: 289–306

Guillaumie S, Pichon M, Martinant JP, Bosio M, Goffner D, Barrière Y (2007) Differential expression of phenylpropanoid and related genes in brown-midrib *bm1, bm2, bm3*, and *bm4* young near-isogenic maize plants. *Planta* 226: 235–250

Halpin C, Holt K, Chojecki J, Oliver D, Chabbert B, Monties B, Edwards K, Barakate A, Foxon GA (1998) *Brown-midrib* maize (*bm1*): a mutation affecting the cinnamyl alcohol dehydrogenase gene. *Plant J* 14: 545–553

Halpin C, Knight ME, Foxon GA, Campbell MM, Boudet AM, Boon JJ, Chabbert B, Tollier M-T, Schuch W (1994) Manipulation of lignin quality of downregulation of cinnamyl alcohol dehydrogenase. *Plant J* 6: 339–350

Hattori T, Murakami S, Mukai M, Yamada T, Hirochika H, Ike M, Tokuyasu K, Suzuki S, Sakamoto M, Umezawa T (2012) Rapid analysis of transgenic rice straw using near-infrared spectroscopy. *Plant Biotechnol* 29: 1–8

He X, Hall MB, Gallo-Meagher M, Smith RL (2003) Improvement of forage quality by downregulation of maize *O*-methyltransferase. *Crop Sci* 43: 2240–2251

Hibino T, Takabe K, Kawazu T, Shibata D, Higuchi T (1995) Increase of cinnamaldehyde groups in lignin of transgenic tobacco plants carrying an antisense gene for cinnamyl alcohol dehydrogenase. *Biosci Biotechnol Biochem* 59: 929–931

Higuchi T, Ito T, Umezawa T, Hibino T, Shibata D (1994) Red-brown color of lignified tissues of transgenic plants with antisense CAD (cinnamyl alcohol dehydrogenase) gene: Wine-red lignin from coniferyl aldehyde. *J Biotechnol* 37: 151–158

Hirano K, Aya K, Kondo M, Okuno A, Morinaka Y, Matsuoka M (2012) *OsCAD2* is the major *CAD* gene responsible for monolignol biosynthesis in rice culm. *Plant Cell Rep* 31: 91–101

Hong L, Qian Q, Tang D, Wang K, Li M, Cheng Z (2012) A mutation in the rice chalcone isomerase gene causes the *golden hull and internode 1* phenotype. *Planta* 236: 141–151

Iwata N, Omura T (1971) Linkage analysis by reciprocal translocation method in rice plants (*Oryza sativa* L.) II Linkage groups corresponding to the chromosomes 5, 6, 8, 9, 10, and 11. *Sci Bull Fac Agric Kyushu Univ* 25: 137–153

Kajita S, Katayama Y, Omori S (1996) Alteration in the biosynthesis of lignin in transgenic plants with chimeric genes for 4-coumarate: Coenzyme A ligase. *Plant Cell Physiol* 37: 957–965

Kim H, Ralph J, Lu F, Pilate G, Leplé J-C, Pollet B, Lapierre C (2002) Identification of the structure and origin of thioacidolysis marker compounds for cinnamyl alcohol dehydrogenase deficiency in angiosperms. *J Biol Chem* 277: 47412–47419

Kim H, Ralph J, Lu F, Ralph SA, Boudet A-M, MacKay JJ, Sederoff RR, Ito T, Kawai S, Ohashi H, et al. (2003) NMR analysis of lignin in CAD-deficient plants Part 1 Incorporation of hydroxycinnamaldehydes and hydroxybenzaldehydes into

lignins. *Org Biomol Chem* 1: 268–281
Kumar A, Hirochika H (2001) Application of retrotransposons as genetic tools in plant biology. *Trends Plant Sci* 6: 127–134
Lai YZ, Sarkanen KV (1971) Isolation and structural studies In: Sarkanen KV, Ludwig CH (eds) *Lignins*. Wiley-Interscience, New York, pp 165–240
Li X, Yang Y, Yao J, Chen G, Li X, Zhang Q, Wu C (2009) *FLXIBLE CULM 1* encoding a cinnamyl-alcohol dehydrogenase controls culm mechanical strength in rice. *Plant Mol Biol* 69: 685–697
MacKay JJ, O'Malley DM, Presnelll T, Booker FL, Campbell MM, Whetten RW, Sederoff RR (1997) Inheritance gene expression and lignin characterization in a mutant pine deficient in cinnamyl alcohol dehydrogenase. *Proc Natl Acad Sci USA* 94: 8255–8260
Miyao A, Tanaka K, Murata K, Sawaki H, Takeda S, Abe K, Shinozuka Y, Onosato K, Hirochika H (2003) Target site specificity of the *Tos17* retrotransposon shows a preference for insertion within genes and against insertion in retrotransposon-rich regions of the genome. *Plant Cell* 15: 1771–1780
Morrow MP, Mascia P, Self KP, Altschuler M (1997) Molecular characterization of a *brown midrib* deletion mutation in maize. *Mol Breed* 3: 351–357
Nakamura Y, Higuchi T (1976) A new synthesis of coniferyl aldehyde and alcohol. *Wood Res.* 59/60: 101–105
Nakatsubo T, Kitamura Y, Sakakibara N, Mizutani M, Hattori T, Sakurai N, Shibata D, Suzuki S, Umezawa T (2008) At5g54160 gene encodes *Arabidopsis thaliana* 5-hydroxyconiferaldehyde *O*-methyltransferase. *J Wood Sci* 54: 312–317
Ookawa T, Tanaka S, Kato H, Hirasawa T (2008) The effect of the decrease in the density of lignin on the lodging resistance of the lignin deficient mutant, *gh2*, in rice. *Jpn J Crop Sci* 77: 210–211 (in Japanese)
Park J-y, Kanda E, Furushima A, Motobayashi K, Nagata K, Kondo M, Ohshita Y, Morita S, Tokuyasu K (2011) Contents of various sources of glucose and fructose in rice straw a potential feedstock for ethanol production in Japan. *Biomass Bioenergy* 35: 3733–3735
Piquemal J, Lapierre C, Myton K, O'Connell A, Schuch W, Grima-Pettenati J, Boudet A-M (1998) Down-regulation of cinnamoyl-CoA reductase induces significant changes of lignin profiles in transgenic tobacco plants. *Plant J* 13: 71–83
Ralph J, Lapierre C, Marita JM, Kim H, Lu F, Hatfield RD, Ralph S, Chapple C, Franke R, Hemm MR, et al. (2001) Elucidation of new structures in lignins of CAD- and COMT-deficient plants by NMR. *Phytochemistry* 57: 993–1003
Saballos A, Vermerris W, Rivera L, Ejeta G (2008) Allelic association, chemical characterization and saccharification properties of *brown midrib* mutants of sorghum (*Sorghum bicolor* (L.) Moench). *Bioenergy Res* 2: 198–204
Saballos A, Ejeta G, Sanchez E, Kang C, Vermerris W (2009) A genomewide analysis of the cinnamyl alcohol dehydrogenase family in sorghum (*Sorghum bicolor* (L.) Moench) identifies *SbCAD2* as the *Brown midrib6* gene. *Genetics* 181: 783–795
Sattler SE, Saathoff AJ, Haas EJ, Palmer NA, Funnell-Harris DL, Sarath G, Pedersen JF (2009) A nonsense mutation in a cinnamyl alcohol dehydrogenase gene is responsible for the sorghum *brown midrib6* phenotype. *Plant Physiol* 150: 584–595
Sattler SE, Funnell-Harris DL, Pedersen JF (2010) Brown midrib mutations and their importance to the utilization of maize sorghum and pearl millet lignocellulosic tissues. *Plant Sci* 178: 229–238
Shiba T, Kubo K, Kawai S (2007) Down regulation of cinnamyl alcohol dehydrogenase (CAD) induces increase of cell wall digestibility in rice (*Oryza sativa*). *Proc 52nd Lignin Symposium*, Utsunomiya, Japan, pp 18–21
Suzuki S, Li L, Sun Y, Chiang VL (2006) The cellulose synthase gene superfamily and biochemical functions of xylem-specific cellulose synthase-like genes in *Populus trichocarpa*. *Plant Physiol* 142: 1233–1245
Suzuki S, Suzuki Y, Yamamoto N, Hattori T, Sakamoto M, Umezawa T (2009) High-throughput determination of thioglycolic acid lignin from rice. *Plant Biotechnol* 26: 337–340
Tsai CJ, Popko JL, Mielke MR, Hu WJ, Podila GK, Chiang VL (1998) Suppression of *O*-methyltransferase gene by homologous sense transgene in quaking aspen causes red-brown wood phenotypes. *Plant Physiol* 117: 101–112
Umezawa T (2010) The cinnamate/monolignol pathway. *Phytochem Rev* 9: 1–17
Van Doorsselaere J, Baucher M, Chognot E, Chabbert B, Tollier M-T, Petit-Conil M, Leplé J-C, Pilate G, Cornu D, Monties B, et al. (1995) A novel lignin in poplar trees with a reduced caffeic acid/5-hydroxyferulic acid *O*-methyltransferase activity. *Plant J* 8: 855–864
Vanholme R, Morreel K, Ralph J, Boerjan W (2008) Lignin engineering. *Curr Opin Plant Biol* 11: 278–285
Vignols F, Rigau J, Torres MA, Capellades M, Puigdomenèch P (1995) The *brown midrib3* (*bm3*) mutation in maize occurs in the gene encoding caffeic acid *O*-methyltransferase. *Plant Cell* 7: 407–416
Weng J-K, Li X, Bonawitz ND, Chapple C (2008) Emerging strategies of lignin engineering and degradation for cellulosic biofuel production. *Curr Opin Biotechnol* 19: 166–172
Yamamura M, Hattori T, Suzuki S, Shibata D, Umezawa T (2010) Microscale alkaline nitrobenzene oxidation method for high-throughput determination of lignin aromatic components. *Plant Biotechnol* 27: 305–310
Yamamura M, Wada S, Sakakibara N, Nakatsubo T, Suzuki S, Hattori T, Takeda M, Sakurai N, Suzuki H, Shibata D, et al. (2011) Occurrence of guaiacyl/*p*-hydroxyphenyl lignin in *Arabidopsis thaliana* T87 cells. *Plant Biotechnol* 28: 1–8
Yamamura M, Noda S, Hattori T, Shino A, Kikuchi J, Takabe K, Tagane S, Gau M, Uwatoko N, Mii M, et al. (2013) Characterization of lignocellulose of *Erianthus arundinaceus* in relation to enzymatic saccharification efficiency. *Plant Biotechnol* 30: 25–35
Zhang K, Qian Q, Huang Z, Wang Y, Li M, Hong L, Zeng D, Gu M, Chu C, Cheng Z (2006) *GOLD HULL AND INTERNODE2* encodes a primarily multifunctional cinnamyl-alcohol dehydrogenase in rice. *Plant Physiol* 140: 972–983
Zhong R, Morrison WH III, Himmelsbach DS, Poole FL II, Ye Z-H (2000) Essential role of caffeoyl Coenzyme A *O*-methyltransferase in lignin biosynthesis in woody poplar plants. *Plant Physiol* 124: 563–577